

## Mode structure of global MHD instabilities and its effect on plasma confinement in LHD

S. Masamune 1), K.Y. Watanabe 2), S. Sakakibara 2), Y. Takemura 1), F. Watanabe 3), S. Ohdachi 2), K. Toi 2), H. Tsuchiya 2), Y. Nagayama 2), Y. Narushima 2) and LHD experiment group 2)

1) Kyoto Institute of Technology, Sakyo-ku, Kyoto 606-8585, Japan

2) National Institute for Fusion Science, Toki, 509-5292, Japan

3) Kyoto University, Sakyo-ku, Kyoto 606-8502, Japan

E-mail contact of main author: masamune@kit.ac.jp

**Abstract.** The LHD magnetic field configuration is characterized by high magnetic shear with low magnetic well or magnetic hill configuration particularly at the plasma periphery. Therefore peripheral  $m=1/n=1$  mode plays important roles in high-beta regime in LHD. In the present study, the  $m=1/n=1$  mode has a resonant surface very close to the outermost flux surface. Relationship between the magnetic fluctuation arising from the mode and internal structure of the mode has been studied using soft-X ray emission profiles. It has been found that the rotating  $m=1/n=1$  mode with magnetic fluctuation level of 0.04%, mode amplitude of 3% and mode width on the major radius normalized to the plasma minor radius of 16% (6% in minor radial direction) brings about 10% degradation of the H factor. The mode amplitude, rather than the magnetic fluctuation amplitude, is shown to be a good parameter in characterizing the effect of the mode on plasma performance.

### 1. Introduction

In the Large Helical Device (LHD), high- $\beta$  plasmas with volume-averaged value of 5% can be sustained for a period of  $\sim 100$  times of the energy confinement time without disruptive phenomena [1]. During the globally stable, long-sustainment phase, it has been observed that magnetic fluctuations due to MHD modes resonant near the plasma periphery, where magnetic hill configuration persists even in high- $\beta$  regimes, have been observed [2]. Although the edge resonant low-order mode does not lead to disruptive discharge termination, there appear fine structures (or local flattening) in density or temperature profiles which may cause degradation of plasma performance. It is therefore quite important to quantitatively identify the effect of the edge-resonant low-order modes on plasma performance for further improvement in the high- $\beta$  plasmas.

In the present study, we will concentrate our attention on the edge resonant  $m=1/n=1$  mode, where  $m$  and  $n$  are the poloidal and toroidal mode numbers of the MHD instability, respectively. Figure 1 shows the dependence of the  $m=1/n=1$  magnetic fluctuation level (fluctuation amplitude normalized to total magnetic field) on the magnetic Reynolds number  $S$  and the volume-averaged beta ( $\langle\beta\rangle$ ) for discharges with  $\langle\beta\rangle$  of up to 5%. It is shown that the fluctuation level is 0.01% for the LHD plasmas with  $\langle\beta\rangle$  of 5%. The magnetic fluctuation level increases as  $\langle\beta\rangle$  increases higher and  $S$  becomes lower. The experimentally

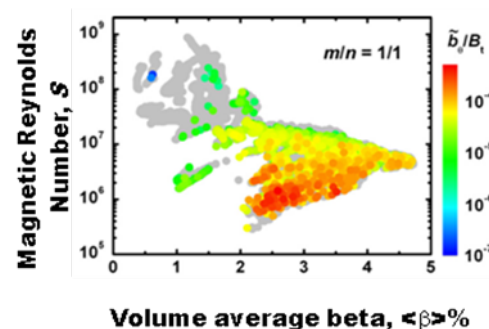


Fig.1 Dependence of magnetic fluctuation level on volume averaged beta  $\langle\beta\rangle$  and magnetic Reynolds number  $S$ .

observed dependence on these two parameters is similar to the theoretical prediction by linear theory of the resistive interchange (resistive g) mode [2]. In the present study, relationship between the magnetic fluctuation arising from the mode and internal structure of the mode has been studied to identify the effect of the mode on plasma performance represented by the  $\beta$  value or H factor. Here the H factor denotes the improvement factor of the confinement time compared with the ISS04 empirical global confinement scaling [3].

In identifying the direct effect of the  $m=1/n=1$  mode on plasma performance, it is of great importance to select discharges which are marginally stable or unstable to the mode. In the present research, we have obtained such LHD discharges in the beta regime of  $\langle \beta \rangle \sim 1\%$  by the change of the pressure gradients and the  $S$  due to the change of the operational magnetic field strength and the induction of the impurity gas-puffing. Here, it should be noted that in the regime of  $\langle \beta \rangle \sim 1\%$ , the  $m=1/n=1$  modes are marginally unstable as shown in Fig.1. In such discharges, the  $m=1/n=1$  magnetic fluctuation appears, or excited fluctuation disappears, in a single discharge. The magnetic fluctuation behaviour is an indication that the discharge is marginally stable or unstable to the  $m=1/n=1$  mode, and the change in plasma performance associated with appearance or disappearance can be regarded as a direct effect of the mode. Internal structure of the mode was studied with soft-X ray (SXR) fluctuation intensity profile, and electron temperature profile by Thomson scattering [4].

## 2. Experimental arrangement and data analysis

The LHD is a heliotron device with a pair of helical coils and three pairs of poloidal coils. All of the coils are superconducting. The typical configuration parameters of the discharges analyzed in this paper are as follows: the major radius is  $\sim 3.75\text{m}$ , the plasma shape in the poloidal cross-section is elliptical, and the length of the major axis is  $\sim 0.8\text{m}$  and the minor axis is  $\sim 1.6\text{m}$ , the central and the edge values of the rotational transform are  $\sim 0.35$  and  $\sim 1.25$ , respectively, and the magnetic shear is strong in the periphery [5].

In the present study, we will characterize the  $m=1/n=1$  mode by three parameters: i) magnetic fluctuation level, ii) SXR fluctuation intensity or mode amplitude, and iii) mode amplitude as full width at half maximum (FWHM) of the SXR fluctuation intensity profile on the major radius. The details of the definitions of these three parameters are as follows.

The  $m=1/n=1$  magnetic fluctuation signals were measured with an array of magnetic probes set on the inner surface of the vacuum vessel. In the present experiment, the  $m=1/n=1$  MHD instability is rotating both toroidally and poloidally at a frequency of several kHz. We have defined the magnetic fluctuation level as follows. A current sheet was assumed on the  $m=1/n=1$  resonant surface and its amplitude was determined such

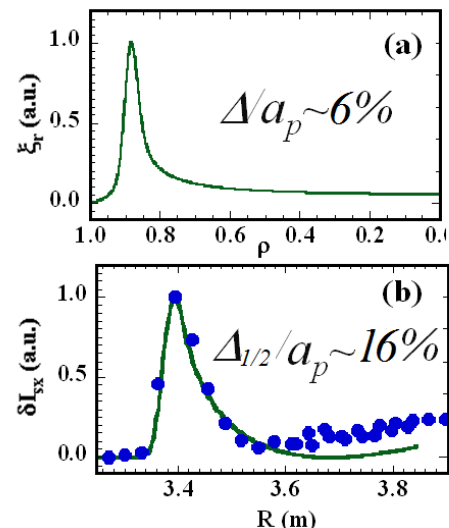


Fig.2: Comparison of major radial profiles of (a) a model eigenfunction of the resistive interchange mode and (b) line-of-sight soft-X ray fluctuation signal. In (b), the solid line is numerical result using the profile in (a) and the circles are experimental results from multi-chord SXR measurement.

that the magnetic fluctuation amplitude (due to the current sheet) agreed with the experimental value at the inner surface of the vacuum vessel. The magnetic fluctuation amplitude (root-mean-square amplitude) at the resonant surface,  $b_{11}$ , was then calculated, and normalized to the total magnetic field intensity  $B_0$ . The normalized amplitude  $b_{11}/B_0$  is called the magnetic fluctuation level. Note that the current sheet model does not necessarily apply to the pressure-driven interchange mode. However, we will use the current sheet model as a reference model which connects the edge magnetic fluctuation amplitude and internal mode structure, that is, mode amplitude and radial width of the mode.

A multi-chord measurement of SXR emission intensity  $I_{SX}$  was performed using two arrays of silicon PIN photodiodes [6], whose vertical sight lines are located in a poloidal cross-section with the vertically elongated plasma shape. The total number of observation chords is 20 for each array, one from torus-outboard side and the other from torus-inboard side. The sampling space is  $\sim 3$ cm on the major radius at the equatorial plane, which corresponds to 7% of the plasma minor radius. In Fig.2, we compare the minor radial profiles of a model eigenfunction of the  $m=1/n=1$  resistive interchange mode (a) and the line-of-sight SXR intensity fluctuation signal ( $\delta I_{SX}$ ) for each line-of-sight from the torus-inboard side (b), where the profiles are shown as functions of the major radius at the equatorial plane. As shown in Fig.2(a), the eigenfunction (local plasma displacement) is well localized at the resonant surface with radial mode width  $\Delta$  of about 6% of the plasma minor radius. Here the local radial mode width  $\Delta$  is defined by the FWHM of the model eigenfunction. The solid line in Fig.2(b) shows the integrated signals of the fluctuating component of the SXR emissivity along each chord with the plasma displacement. The filled circles in Fig.2(b) are the experimental results, showing good agreement. The good agreement indicates that we can identify correspondence between the radial width of the mode and the structure of SXR fluctuation profile.

Here it should be noticed that the FWHM of the local plasma displacement normalized to the plasma minor radius  $a_p$  of 6% corresponds to the FWHM of line-integrated SXR fluctuation  $\delta I_{SX}$  profile normalized to  $a_p$  of 16% as shown in Fig.2(b). Moreover, due to the divergent angle of the sight lines of the SXR detector array, the mode width in the local cannot be identified for the modes with less than 5% of FWHM in the local. And we should note that in the present experiments, the magnetic axis was located at  $R=3.9$ m, so, the number of outer chords of the magnetic axis is not large enough to obtain good spatial resolution for identification of the mode structure.

Estimate of the confinement property was carried out with the help of ISS04 scaling. As for the plasma  $\beta$  value, the experimental  $\langle \beta \rangle$  from diamagnetic measurement was compared with  $\beta$  value from ISS04 scaling value. Similar comparison has also been carried out for H factor as follows. H factor was estimated by

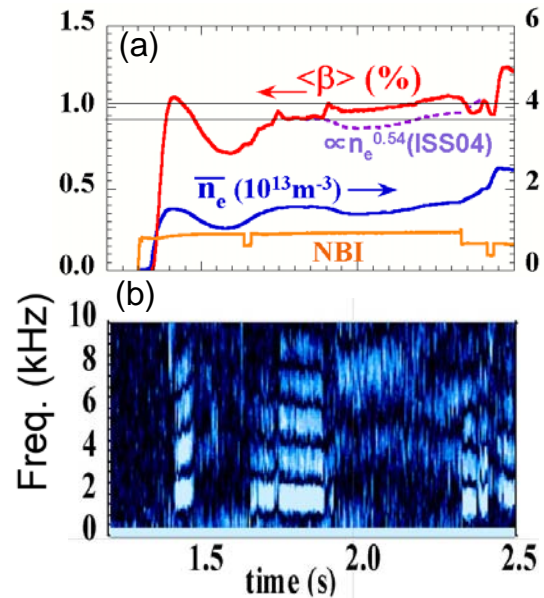


Fig.3: An example of a LHD discharge analyzed in the present study. The magnetic fluctuation due to low-order  $m=1/n=1$  peripheral MHD mode disappears during the discharge, the disappearance being accompanied by the recovery of confinement properties.

two methods using ISS04 scaling: one estimated from plasma parameters at a time when the  $m=1/n=1$  mode is absent, and the other estimated from instantaneous plasma parameters before or after disappearance of the  $m=1/n=1$  mode. The ratio  $H_{ISS04}/H_{ISS04at^{**s}}$  is used as a measure of the change in confinement properties brought about by the  $m=1/n=1$  mode.

### 3. $m=1/n=1$ mode behavior and associated change in confinement property

An example of a set of signals in a discharge where the edge resonant  $m=1/n=1$  mode appears and disappears is given in Fig.3. Figure 3(a) shows the time evolutions of the  $\langle\beta\rangle$ , the line averaged electron density and the NBI port-through power. The beta value is obtained from the diamagnetic measurement. Figure 3(b) shows time evolution of the coherence of the magnetic fluctuation as a function of the frequency. The white region corresponds to the existence of the coherent modes. Before 1.9s, the strong coherent modes are observed in  $\sim 1.7\text{kHz}$ ,  $\sim 3.5\text{kHz}$ ,  $\sim 5\text{kHz}$  and so on, which correspond to  $m/n=1/1$ ,  $2/2$ ,  $3/3$ , ... according to the mode analysis with the magnetic probe array. Here it should be noted that the power spectrum of  $m/n=1/1$  mode is much larger than that of the other modes. The abrupt increase (recovery) of  $\langle\beta\rangle$  is observed when the coherent magnetic fluctuations disappear at  $\sim 1.9\text{s}$ .

The dashed line corresponds to the predicted beta value as to keep the same confinement property based on the ISS04 scaling as that before the MHD activity disappears. From Fig.3(a), the plasma confinement property is degraded by 5% in the plasma stored energy due to the existence of the coherent magnetic fluctuation.

From the above effect of the MHD fluctuation on the plasma confinement property, it is essential to obtain the relationship between the internal structure of the mode and its effect on plasma confinement. The mode structure before the disappearance of the  $m=1/n=1$  magnetic fluctuation was obtained from the soft-X ray (SXR) fluctuation. The SXR fluctuation component coherent with the  $m=1/n=1$  magnetic fluctuation was extracted. Figure 4 shows the major radial profiles of the rotational transform and fluctuation amplitude of the line integrated SXR emission intensity just before the disappearance of the  $1/1$  mode shown in Fig.3, which correspond to the filled symbols in Fig.2(b). Figure 5 shows the phase profile, indicating that the fluctuation is odd in poloidal mode number and that the phase does not change across the  $m=1/n=1$  resonant surface. The latter is the characteristic of the pressure-driven instability which produces no current sheet on the resonant surface. From this line integrated SXR fluctuation profile we can define the line-integrated mode width  $\Delta_{1/2}$  as the FWHM from the torus-inboard profile as described in the previous section. In the case of Fig.4, the radial mode width normalized to  $a_p$  is  $\sim 6\%$  and normalized line-integrated mode width (also normalized to  $a_p$ ) is  $\sim 16\%$ , as shown in the previous section.

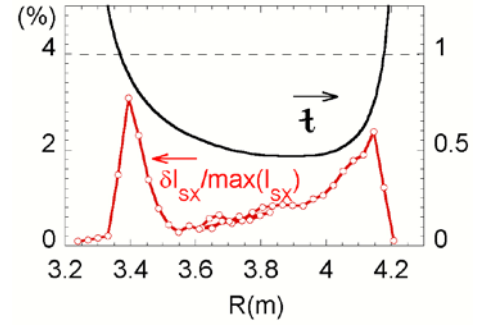


Fig.4: Major radial profiles of the rotational transform and SXR amplitude coherent with the  $m=1/n=1$  magnetic fluctuation at  $t=1.8\text{s}$  in Fig.3.

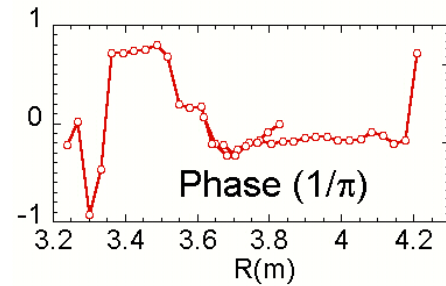


Fig.5: Major radial profiles of the phase of SXR fluctuation indicating odd mode. No significant change in phase is observed across the resonant surface.

#### 4. Mode structure, edge magnetic fluctuation and their effects on confinement

We will describe the dependence of plasma performance on magnetic fluctuation and SXR fluctuation, and discuss that SXR fluctuation amplitude is a good parameter to characterize the improvement or degradation of the plasma performance.

In Fig.6, three different discharges are shown to see the dependence on magnetic fluctuation level of confinement degradation evaluated from time evolution of the normalized H factor. In Fig.6(a), where magnetic fluctuation level is 0.008%, appearance of the  $m=1/n=1$  mode at  $t=2.69$  s does not cause any degradation of the H factor. When the fluctuation level increased to  $\sim 0.04\%$ , as shown in Fig.6(b), the H factor was degraded by  $\sim 5\%$  as the mode appears. In this case, the total magnetic field intensity  $B_0$  was 1.375T, lower than the case in Fig.6(a) with  $B_0$  of 1.75T. And  $\langle\beta\rangle$  in Fig.6(b) was  $\sim 0.5\%$ , lower than the case in Fig.6(a) with  $\langle\beta\rangle\sim 1\%$ . In Fig.6(c), the  $m=1/n=1$  mode brought about further degradation, up to 10%. In this case, the magnetic fluctuation level was almost the same as in Fig.6(b), but with lower  $B_0$  of 0.9T and higher  $\langle\beta\rangle\sim 1\%$ .

In Fig.7, the SXR fluctuation intensity profiles are shown in the three cases in Fig.6. The total magnetic field intensity  $B_0$  is chosen as a parameter in this figure. In the case of  $B_0=1.75$ T shown by the green line, the internal structure of the mode can be identified in the SXR fluctuation intensity profile, however, it is difficult to define the line-integrated mode width precisely because the maximum fluctuation signal is too low. The SXR fluctuation increased to 1.5% with  $B_0$  of 1.375T as shown by the blue line. In this case, as shown in Fig.6(b), the magnetic fluctuation level was  $\sim 0.04\%$ . When the magnetic field was decreased to  $B_0=0.9$ T, the SXR fluctuation intensity increased further to  $\sim 3\%$  as shown by the red line, while the magnetic fluctuation level did not change significantly from the case with  $B_0=1.375$ T. The relationship between the SXR fluctuation intensity (or mode amplitude) and the magnetic fluctuation level is not linear when the change in total field intensity  $B_0$  is taken into account.

Figure 8 shows the relationship between the SXR fluctuation intensity and the magnetic

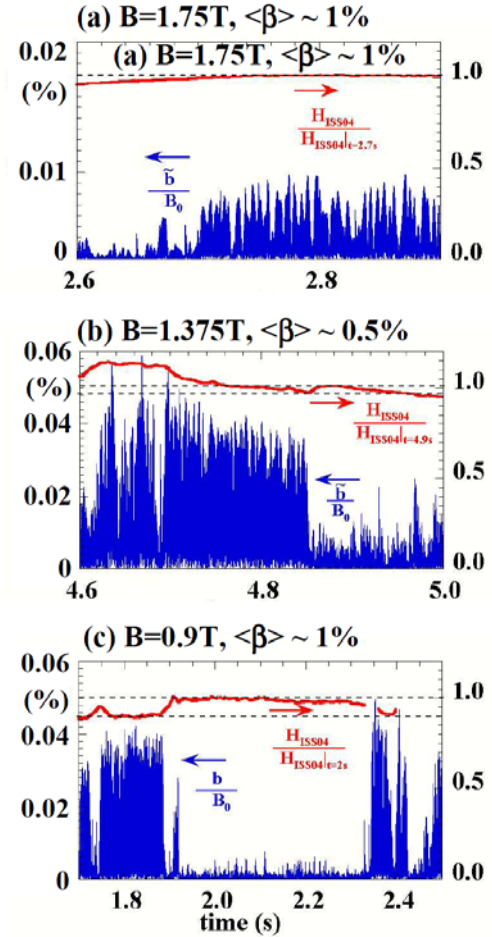


Fig.6: Effect of  $m=1/n=1$  magnetic fluctuation level on confinement degradation.

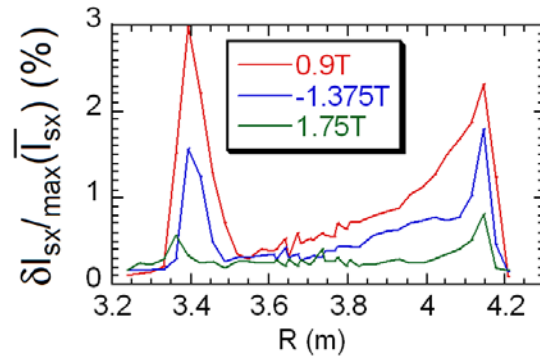


Fig7: Dependence of SXR fluctuation profile on total magnetic field intensity  $B_0$ .

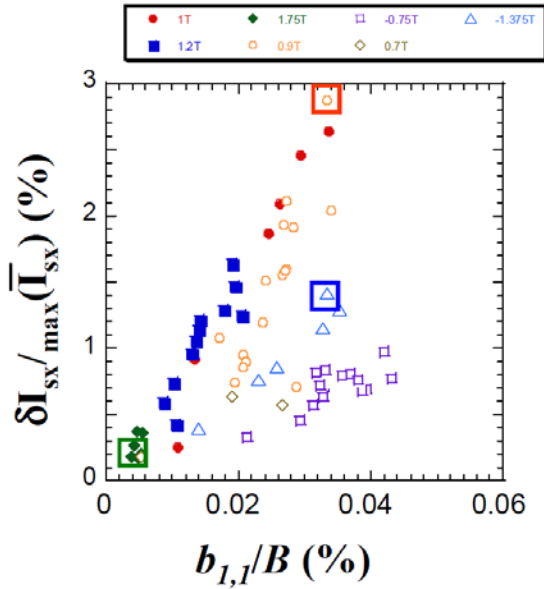


Fig.8: Dependence of SXR fluctuation amplitude on magnetic fluctuation level.

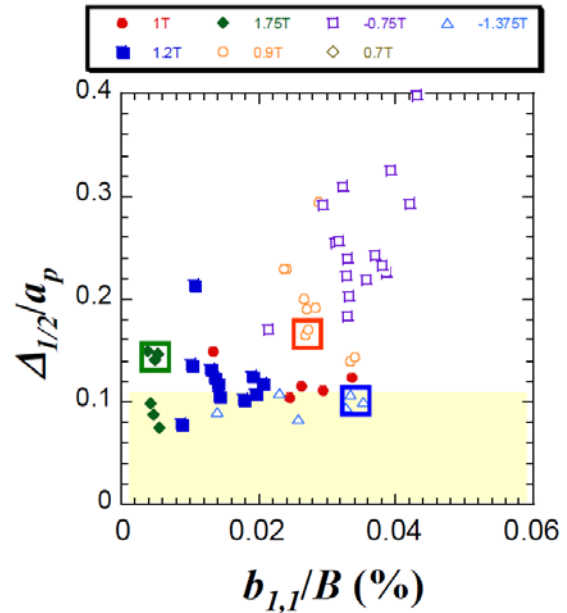


Fig.9: Relationship between the mode width estimated from the SXR fluctuation profile and magnetic fluctuation level.

fluctuation level with  $B_0$  being the parameter.

The green, the blue and the red squares in Fig.8 correspond to Fig.6(a), (b) and (c), respectively. The figure shows that the SXR fluctuation intensity increased almost linearly with an increase in magnetic fluctuation level for a fixed value of  $B_0$ . However, the gradient changes when we change the value of  $B_0$ . Higher gradient results for lower magnetic field, indicating the dependence of other parameters such as the magnetic Reynolds number  $S$ . The mode width also expands with an increase in magnetic fluctuation level as shown in Fig.9. In the region where the normalized line-integrated mode width is less than 10% (shaded region), it is difficult to define the mode width from the major radial profile of the SXR fluctuation intensity because of the finite divergent angles of the SXR sight lines as discussed in section 2. We can conclude that when the line-integrated mode width normalized to the plasma minor radius increased to 10% or higher, we can identify the degradation of plasma performance. The degree of degradation represented by the change in H factor is proportional to the mode amplitude, rather than the magnetic fluctuation level, when we take into account the magnetic field intensity  $B_0$  as an operational parameter. Therefore, we conclude that the mode amplitude, estimated from the SXR fluctuation intensity profile, is a good parameter which characterizes the effect of the  $m=1/n=1$  mode on degradation of the plasma performance.

## 5. Discussion

In this section we will discuss how the internal electron temperature profile changes when the confinement property is degraded. In Fig.10, we compare the radial profiles of decrement in electron temperature caused by the presence of the  $m=1/n=1$  mode in the case of  $B_0=0.9T$  as shown in Fig.3. In this case the  $m=1/n=1$  mode with normalized amplitude of 3% and magnetic fluctuation

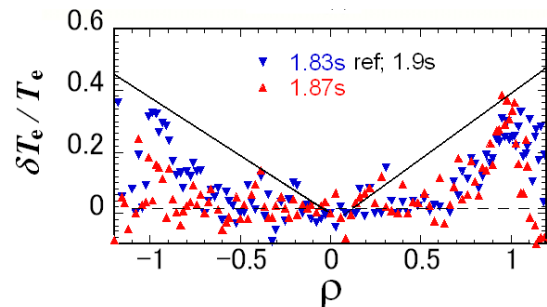


Fig.10: Radial profile of decrement in electron temperature associated with the presence of the 1/1 mode.

level of 0.04% disappears at  $t=1.9s$ . The electron temperature profiles well before the disappearance ( $t=1.83s$ ) and just before the disappearance ( $t=1.87s$ ) were compared with the profile just after the disappearance ( $t=1.9s$ ) of the  $m=1/n=1$  mode. The result shows that the decrease in electron temperature is restricted to the peripheral region where the  $m=1/n=1$  mode amplitude has substantial value, and the decrease in the hot core region cannot be observed. For the  $m=1/n=1$  mode with amplitude less than 3%, the mode does not have influence in the hot core region.

The  $m=1/n=1$  mode amplitude is a good parameter to characterize the effect of the mode on the degree of confinement degradation. In terms of the H factor, we can summarize the results in Figs. 6 and 7 as follows. The H factor was degraded by 10% by the presence of the  $m=1/n=1$  mode with amplitude of 3%, and 5% degradation was observed when the mode amplitude was 1.5%, while no degradation was observed when the mode amplitude was  $\sim 0.4\%$ . The effect of mode width, both radial and line-integrated, on confinement degradation has not become clear yet. We need internal mode structure to evaluate the effect of mode width, and higher spatial resolution of the SXR fluctuation profiles on the equatorial plane is required for that purpose. Improvement of spatial resolution is needed particularly of the SXR detector array for the torus outboard side sight lines.

The present result would be helpful in understanding the relationship between the internal structure of the  $m=1/n=1$  mode and associated change in radial profiles of plasma parameters. The observed relationship between the experimentally measured magnetic fluctuation level and the  $m=1/n=1$  mode amplitude and width would work as a basic data base for active control of the peripheral low-order mode.

## 6. Conclusion

Toroidally and poloidally rotating low-order peripheral mode is frequently observed in high-beta LHD discharges. Experimental studies have been carried out to quantitatively evaluate the effect of the  $m=1/n=1$  peripheral mode on the plasma confinement performance using the LHD discharges which are marginally stable or unstable to the  $m=1/n=1$  mode, in the range of magnetic fluctuation level up to 0.04%.

The degradation of the confinement performance is caused by decreased edge electron temperature where resonant surface of the mode exists. We can make the following quantitative evaluation of the effect of the mode in terms the magnetic fluctuation level; The rotating  $m=1/n=1$  mode magnetic fluctuation level of 0.04%, the mode amplitude of 3% and line-integrated mode width of 15% (6% in minor radial direction) brings about 10% degradation of confinement performance characterized by the H factor. It was found that the maximum intensity of SXR fluctuation profile in the equatorial plane, corresponding to the  $m=1/n=1$  mode amplitude, is a good parameter to characterize the effect of the mode on the confinement performance. The H factor was degraded by 10% by the presence of the  $m=1/n=1$  mode with amplitude of 3%, and 5% degradation of H factor was observed when the mode amplitude was 1.5%. No degradation was observed when the mode amplitude was  $\sim 0.4\%$ .

The present result would be helpful in understanding the role of edge resonant low order edge resonant modes in confinement performance of high beta LHD plasmas. It would also work as a basic data base for active control of the peripheral low-order mode.

## Acknowledgements

The authors are grateful to the LHD operation group for their technical support. This work is supported by the budget NIFS07KOA022 of the National Institute for Fusion Science.

## References

- [1] A. Komori et al., Nucl. Fusion 49 (2009) 104015.
- [2] S. Sakakibara et al., Plasma Phys. Control. Fusion 50 (2008) 124014.
- [3] H. YAMADA et al., Nucl. Fusion, 45 (2005) 1684.
- [4] I. Yamada et al., Fusion Sci. Technol. 58 (2010) 345.
- [5] K.Y. Watanabe et al., Fusion Sci. Technol. 58 (2010) 160.
- [6] S. Ohdachi et al., Fusion Sci. Technol. 58 (2010) 418.